Neither Classical nor Alternative Macrophage Activation Is Required for *Pneumocystis* Clearance during Immune Reconstitution Inflammatory Syndrome

Zhuo-Qian Zhang,[a] Jing Wang,[b] Zachary Hoy,[b] Achsah Keegan,[c] Samir Bhagwat,[b] Francis Gigliotti,[a,b] Terry W. Wright[a,b]

Department of Microbiology and Immunology[a] and Department of Pediatrics,[b] University of Rochester School of Medicine and Dentistry, Rochester, New York, USA; Center for Vascular and Inflammatory Diseases, Department of Microbiology and Immunology, University of Maryland School of Medicine, Baltimore, Maryland, USA[c]

Pneumocystis is a respiratory fungal pathogen that causes pneumonia (*Pneumocystis* pneumonia [PcP]) in immunocompromised patients. Alveolar macrophages are critical effectors for CD4$^+$ T cell-dependent clearance of *Pneumocystis*, and previous studies found that alternative macrophage activation accelerates fungal clearance during PcP-related immune reconstitution inflammatory syndrome (IRIS). However, the requirement for either classically or alternatively activated macrophages for *Pneumocystis* clearance has not been determined. Therefore, RAG2$^{-/-}$ mice lacking either the interferon gamma (IFN-γ) receptor (IFN-γR) or interleukin 4 receptor alpha (IL-4Rα) were infected with *Pneumocystis*. These mice were then immune reconstituted with wild-type lymphocytes to preserve the normal T helper response while preventing downstream effects of Th1 or Th2 effector cytokines on macrophage polarization. As expected, RAG2$^{-/-}$ mice developed severe disease but effectively cleared *Pneumocystis* and resolved IRIS. Neither RAG/IFN-γR$^{-/-}$ nor RAG/IL-4Rα$^{-/-}$ mice displayed impaired *Pneumocystis* clearance. However, RAG/IFN-γR$^{-/-}$ mice developed a dysregulated immune response, with exacerbated IRIS and greater pulmonary function deficits than those in RAG2 and RAG/IL-4Rα$^{-/-}$ mice. RAG/IFN-γR$^{-/-}$ mice had elevated numbers of lung CD4$^+$ T cells, neutrophils, eosinophils, and NK cells but severely depressed numbers of lung CD8$^+$ T suppressor cells. Impaired lung CD8$^+$ T cell responses in RAG/IFN-γR$^{-/-}$ mice were associated with elevated lung IFN-γ levels, and neutralization of IFN-γ restored the CD8 response. These data demonstrate that restricting the ability of macrophages to polarize in response to Th1 or Th2 cytokines does not impair *Pneumocystis* clearance. However, a cell type-specific IFN-γ/IFN-γR-dependent mechanism regulates CD8$^+$ T suppressor cell recruitment, limits immunopathogenesis, preserves lung function, and enhances the resolution of PcP-related IRIS.

Pneumocystis is an opportunistic fungal pathogen, which is widespread throughout the human population. Vargas et al. reported that nearly 85% of children have been exposed to *Pneumocystis* by 20 months of age (1). The infection appears mild and self-limited in a normal host, but *Pneumocystis* causes life-threatening pneumonia in patients with defects in cell-mediated immunity. *Pneumocystis* pneumonia (PcP) remains prevalent in those with AIDS (2) and is a leading cause of death in HIV-infected patients, with a mortality rate of up to 50% in those with severe disease (3). *Pneumocystis* also infects patients receiving long-term immunomodulatory therapy for rheumatoid arthritis and other inflammatory diseases (4) as well as cancer patients undergoing chemotherapy (5). Furthermore, *Pneumocystis* infection or colonization has been associated with chronic obstructive pulmonary disease in both HIV and non-HIV patients (6).

Despite the availability of antibiotics that effectively eradicate *Pneumocystis*, rapid clinical improvement is not always observed in patients with PcP. The host's immune response against this pathogen often contributes to severe PcP-related lung injury (6, 7). Clinical studies suggest that the intensity of pulmonary inflammation, rather than organism lung burden, correlates with the severity of PcP (8–10). Furthermore, rapid and unbalanced restoration of cell-mediated immunity following antiretroviral treatment of *Pneumocystis*-infected HIV patients sometimes results in exaggerated lung inflammation and leads to the clinical manifestation of immune reconstitution inflammatory syndrome (IRIS) (11). IRIS is an example of the immunopathogenic nature of PcP, in which the restoration of adaptive immune function brings

about a rapid and intense T cell response that clears the organism but also inflicts significant lung damage (12).

T cells are critical for host defense against *Pneumocystis* (13–16). The downstream effector mechanisms through which T cells clear *Pneumocystis* have been linked to distinct alveolar macrophage (AM) phenotypes. Interferon gamma (IFN-γ), a soluble cytokine produced by CD4$^+$ T helper 1 (Th1) cells, converts resting macrophages into cells with proinflammatory properties. These cells are known as classically activated or M1 macrophages (17, 18). CD4$^+$ T helper 2 (Th2) responses produce the cytokines interleukin 4 (IL-4) and interleukin 13 (IL-13), which share the IL-4 receptor alpha (IL-4Rα) subunit (19, 20). In contrast to M1 phenotype macrophages, IL-4 and IL-13 induce an alternatively activated macrophage phenotype (M2) with anti-inflammatory properties (21). M1 and M2 macrophages differ in their abilities to
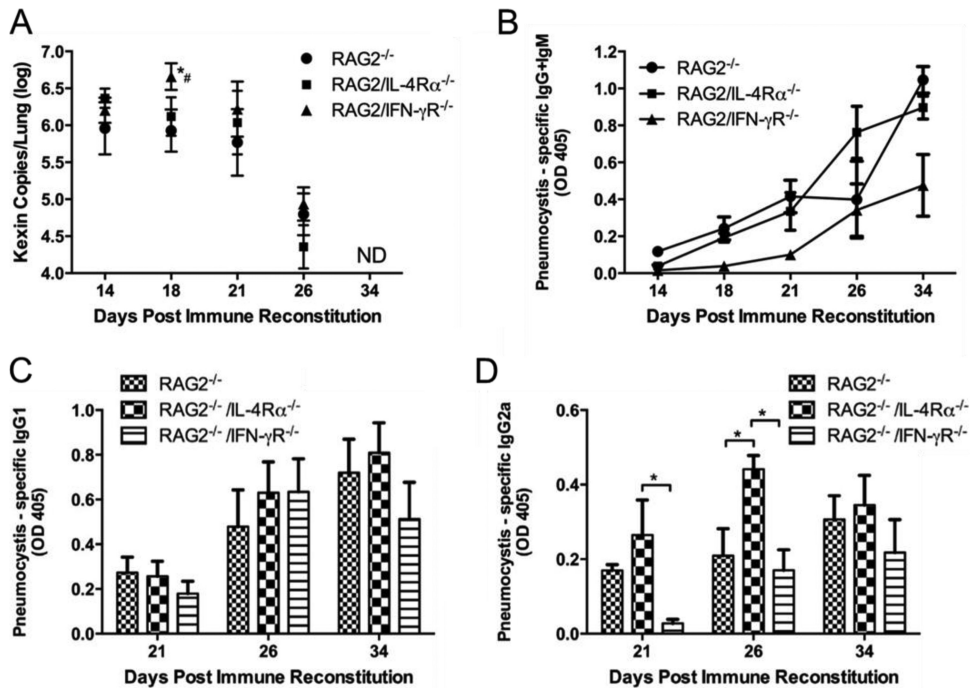
FIG 1 Blockade of classical or alternative macrophage polarization does not affect *Pneumocystis* clearance or development of anti-*Pneumocystis* antibodies. (A) *Pneumocystis* burden in the lungs of RAG2$^{-/-}$, RAG2/IL-4R$\alpha$$^{-/-}$, and RAG2/IFN-$\gamma$R$^{-/-}$ mice was measured by real-time PCR quantitation of *Pneumocystis kexin* gene copy numbers in lung homogenates at days 14, 18, 21, 26, and 34 post-immune reconstitution. Values are means $\pm$ 1 standard error ($n = 6$ to 10 per group at each time point). Data represent results from at least two independent experiments. *, $P < 0.05$ compared to RAG2$^{-/-}$ mice; #, $P < 0.05$ compared to RAG2/IL-4R$\alpha$$^{-/-}$ mice. ND indicates that no signal was detected in any mice at that time. *Pneumocystis*-specific IgG and IgM (B), IgG1 (C), and IgG2a (D) antibodies in *Pneumocystis*-infected RAG2$^{-/-}$, RAG2/IL-4R$\alpha$$^{-/-}$, and RAG2/IFN-$\gamma$R$^{-/-}$ mouse sera were measured by an ELISA using soluble *Pneumocystis* antigen from infected mouse lung homogenates as the target. OD, optical density. *, $P < 0.05$ compared to the indicated group.

contribute to host defense against specific classes of pathogens. Our laboratory previously demonstrated that treatment with the immunomodulatory agent sulfasalazine (SSZ) reduced PcP-related immunopathogenesis and accelerated organism clearance. The beneficial effects of SSZ were associated with an increase in the abundance of macrophages with the M2 phenotype and enhanced AM phagocytosis of *Pneumocystis* (18). Other groups have also found that Th2 and M2 macrophages are effector cells that mediate immunity to *Pneumocystis* infection (22).

The purpose of this study was to determine whether restricting M1 or M2 macrophage polarization alters the host's immune response to *Pneumocystis*. The immune-reconstituted immunodeficient mouse model of PcP is very similar to the clinical presentation of PcP-related IRIS (14, 23) and has been used successfully to study both fungal clearance as well as PcP-related immunopathogenesis. To study the effects of altering the host's capacity to polarize M1 or M2 macrophages, recombination-activating gene 2 (RAG2) knockout mice, which lack mature lymphocytes (24), were crossed with IFN-γ receptor (IFN-γR)- or IL-4Rα-deficient mice. The resulting transgenic strains were immunodeficient and impaired in their ability to polarize either M1 or M2 macrophages due to the lack of IFN-γR or IL-4Rα, respectively. Immune reconstitution of these mice with wild-type splenocytes allowed for the preservation of the T helper balance but blocked the ability of Th1 and Th2 effector cytokines to modify macrophage phenotype and function.

MATERIALS AND METHODS

Mice. Severe combined immunodeficient (SCID) mice on a C.B-17 background were obtained from a breeding colony at the University of Rochester. Mice were housed in a sterilized environment using microisolator technology. SCID mice were cohoused with *Pneumocystis*-infected SCID mice to induce infection. *Pneumocystis* organisms were isolated as previously described (25). *Pneumocystis* cysts were enumerated by using standard Gomori's methenamine silver (GMS) stain. BALB/c and RAG2-deficient mice were purchased from Taconic Biosciences (Germantown, NY). BALB/c IFN-γR$^{-/-}$ mice were purchased from The Jackson Laboratory (Bar Harbor, ME). RAG2/IL-4R$\alpha$$^{-/-}$ mice (described in reference 26) were obtained from the University of Maryland and bred at the University of Rochester. RAG2/IFN-γR$^{-/-}$ mice were generated by crossing IFN-γR$^{-/-}$ mice onto the RAG2$^{-/-}$ background. All experimental mice were on the BALB/c background. The University Committee for Animal Research (UCAR) at the University of Rochester Medical Center approved all animal protocols.

Model of PcP-related IRIS. The mouse model of PcP-related IRIS was used, as described previously (18, 27). RAG2$^{-/-}$, RAG2/IL-4R$\alpha$$^{-/-}$, and RAG2/IFN-$\gamma$R$^{-/-}$ mice were intratracheally inoculated with 5×10^5 purified *Pneumocystis* organisms based on cyst counts. At 3 weeks postinoculation, the mice were immune reconstituted with 5×10^7 wild-type lymphocytes isolated from the spleens of BALB/c mice.

Physiological assessment of live and ventilated mice. Dynamic lung compliance and lung resistance were measured in live, ventilated mice by using a whole-body plethysmograph (Buxco Electronics Inc., Wilmington, NC) connected to a Harvard rodent ventilator (Harvard Apparatus, Southnatic, MA), as described previously (18, 27). Respiratory rates were measured by using whole-body unrestrained chambers, and data were
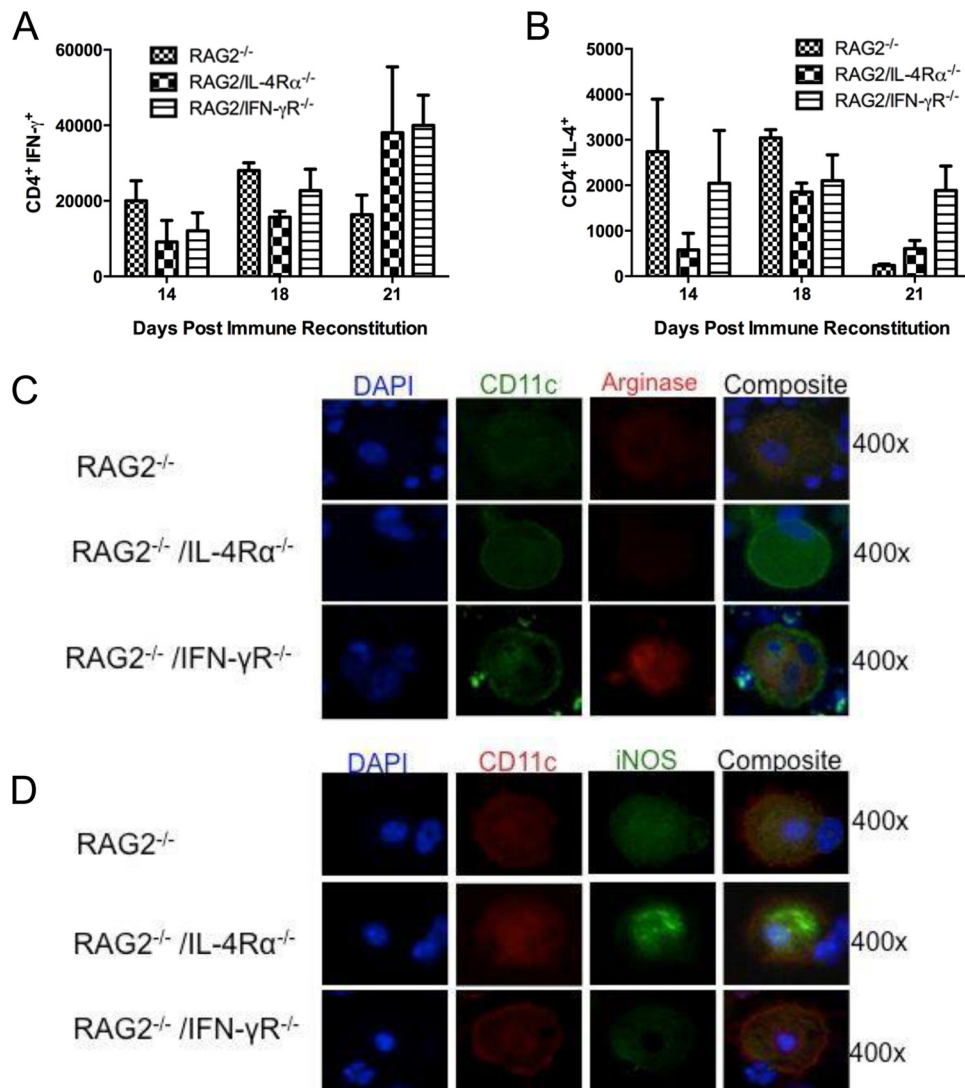
FIG 2 Impaired alveolar macrophage polarization in RAG2/IL-4Rα$^{-/-}$ and RAG2/IFN-γR$^{-/-}$ mice. (A and B) BAL fluid cells were collected from immune-reconstituted, *Pneumocystis*-infected RAG2$^{-/-}$, RAG2/IL-4Rα$^{-/-}$, and RAG2/IFN-γR$^{-/-}$ mice and stimulated with PMA and ionomycin. Total numbers of CD4^{+} T cells producing IFN-γ and IL-4 were determined by intracellular cytokine staining. Values are means ± 1 standard error ($n = 3$ to 5 per group at each time point). (C and D) BAL fluid cells were collected from *Pneumocystis*-infected RAG2$^{-/-}$, RAG2/IL-4Rα$^{-/-}$, and RAG2/IFN-γR$^{-/-}$ mice at day 18 post-immune reconstitution. (C) Cells were stained with antibodies specific for the alveolar macrophage marker CD11c (green) and arginase (red). (D) Cells were also stained with antibodies specific for CD11c (red) and iNOS (green). Nuclei were stained with DAPI (blue). At least 200 CD11c^{+} cells were examined for each strain. Magnification, ×400.

collected and analyzed by using the Biosystems XA software package (Buxco Electronics Inc.).

Bronchoalveolar lavage. The lungs of individual mice were lavaged with four 1-ml aliquots of ice-cold 1× Hanks' balanced salt solution. The lavage cells were recovered by centrifugation, and the cell-free bronchoalveolar lavage (BAL) fluid was immediately frozen at −80°C. The recovered cells were resuspended in RPMI 1640 medium supplemented with 20% fetal bovine serum (FBS), 2% L-glutamine, 1% penicillin and streptomycin, 1% sodium pyruvate, 20 mM HEPES, and 2-mercaptoethanol (all reagents were purchased from Life Technologies). Cell aliquots were taken for total cell counts and differential staining.

Flow cytometry. Unstimulated BAL fluid cells were incubated with Fc block (BD Biosciences, San Diego, CA) and then with fluorescently labeled antibodies against the surface markers CD4 (RM4-5), CD8 (53-6.7), CD11c (HL3), GR-1 (RB6-8C5), and CD3 (500A2). Some BAL fluid cells were stimulated with 50 to 100 ng/ml phorbol myristate

acetate (PMA) and 1 mM ionomycin for 4 h in the presence of Golgi-Plug (BD Biosciences), as described previously (27). Stimulated cells were incubated with Live/Dead Fixable Aqua stain (Molecular Probes, Eugene, OR) for 30 min, followed by surface staining. Cytofix/Cytoperm kit (BD) reagents and directions were used for subsequent fixation and permeabilization steps. Antibodies for IFN-γ (XMG1.2; eBioscience, San Diego, CA), IL-4 (11B11; eBioscience), and Foxp3 were used for intracellular staining. Cells were analyzed by using a BD LSR II flow cytometer with BD FACSDiva software, and analyses were performed with FlowJo (Tree Star, Ashland, OR).

Detection of anti-*Pneumocystis* serum antibodies. Anti-*Pneumocystis* antibodies in serum samples from experimental mice were measured as previously described (28, 29). Briefly, flat-bottom microtiter plates (ICM Biomedical, Aurora, OH) were coated overnight with mouse *Pneumocystis* antigen (in 0.05 M carbonate buffer, pH 9.6) at room temperature. The plates were then washed and incubated for 2 h in 5% powdered milk in
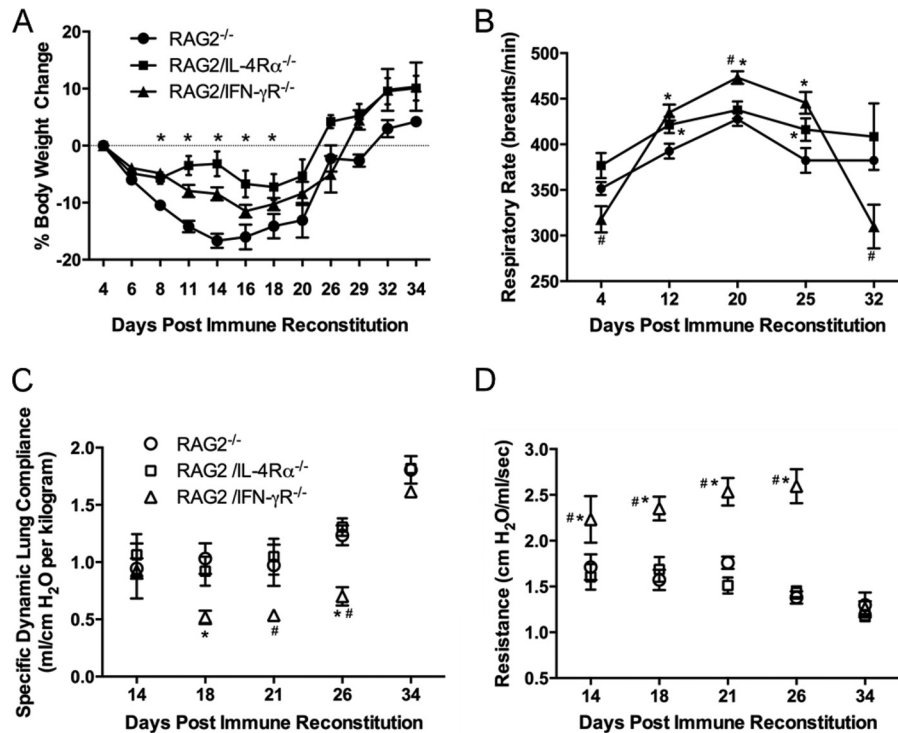
FIG 3 Loss of IFN-γR signaling is associated with greater pulmonary function deficits and increased lung injury. Physiological measurements of lung function in *Pneumocystis*-infected immune-reconstituted RAG2$^{-/-}$, RAG2/IL-4Rα$^{-/-}$, and RAG2/IFN-γR$^{-/-}$ mice were performed. Body weights (A) and respiratory rates (B) were monitored noninvasively over a 27-day period postreconstitution. Specific dynamic lung compliance (C) and lung resistance (D) measurements were performed post-immune reconstitution on anesthetized mice placed in a whole-body plethysmography chamber. Values are means ± 1 standard error ($n = 6$ to 10 per group at each time point). Data represent results from at least two independent experiments. *, $P < 0.05$ compared to RAG2$^{-/-}$ mice; #, $P < 0.05$ compared to RAG2/IL-4Rα$^{-/-}$ mice.

phosphate-buffered saline (PBS). Mouse sera were diluted 1:50 in PBS plus 0.1% Tween and incubated on coated plates for 2 h at 37°C. After washing, the plates were incubated with alkaline phosphatase-conjugated secondary antibodies for 1 h at 37°C. Secondary anti-mouse IgG and IgM, IgM, IgG1, IgG2a, or IgG2b were used to define the Ig subtypes produced (Jackson ImmunoResearch Laboratories, West Grove, PA). After washing, a chromogenic substrate was added, and the optical density was read with a SpectraMax M5 microplate reader and analyzed with SoftPro Max 5.2 software (Molecular Devices, Sunnyvale, CA). Controls included hyperimmune sera of immunocompetent mice immunized with whole *Pneumocystis* organisms. Samples were also tested against noninfected normal lung antigen preparations for data normalization.

Lung cytokine ELISAs. Lungs were collected and homogenized in PBS. Lung homogenates were centrifuged at 250 × *g* to remove cell debris and stored at −80°C. IL-4 and IFN-γ levels were measured by using commercially available enzyme-linked immunosorbent assay (ELISA) kits (R&D Systems, Minneapolis, MN).

Assessment of *Pneumocystis* lung burden. Since *Pneumocystis* cannot be reliably cultured, a real-time PCR method was used to quantify lung burden, as previously described (18). For quantification of *Pneumocystis* burden in right lung lobes, quantitative PCR using TaqMan primer/fluorogenic probe chemistry and an Applied Biosystems Prism 7000 sequence detection system (Applied Biosystems, Foster City, CA) was performed with a primer/probe set specific for the mouse single-copy *Pneumocystis kexin* gene.

Histology. The lungs of some experimental mice were inflated with 15-cm gravity flow pressure with 10% formalin (Sigma, St. Louis, MO). The lungs were fixed *in situ* for 10 min, removed from the chest, placed into a fixative solution at room temperature overnight, and then washed with 70% ethanol the following day. Lung tissue was then embedded in

paraffin, and 4-μm sections were cut and stained with hematoxylin and eosin for visualization.

Assessment of alveolar macrophage phenotype. The alveolar macrophage phenotype was determined by using immunofluorescence staining of inducible nitric oxide synthase (iNOS) and arginase, as previously described (18). BAL fluid cells from whole-lung lavage fluid were centrifuged onto glass slides. Cells were fixed with 3% paraformaldehyde and then permeabilized with 0.2% Triton X-100 in PBS for 15 min. Following permeabilization, the cells were stained with either primary rabbit anti-mouse iNOS (Abcam, MA) plus secondary goat anti-rabbit Alexa Fluor 488 (AF488) (Invitrogen Molecular Probes, OR) or primary goat anti-mouse arginase (Santa Cruz Biotechnology, CA) with secondary donkey anti-goat AF546 (Invitrogen Molecular Probes, OR). Cells were then stained with hamster anti-mouse CD11c (Abcam, MA), followed by either goat anti-hamster AF594 or goat anti-hamster AF488 (Invitrogen Molecular Probes, OR) secondary antibody. All cells were then stained with 4′,6-diamidino-2-phenylindole (DAPI) nuclear stain. After staining, slides were mounted with antifade Vectashield (Vector Laboratories, CA). A Nikon Eclipse E400 fluorescence microscope was used for photomicroscopy. All photographs for a given protein were taken with identical exposure settings.

Statistical analyses. Differences between experimental groups at different doses or at different time points were analyzed by using analysis of variance (ANOVA) with Bonferroni's multiple-comparison posttest. Differences were considered significant at P values of <0.05. All data were analyzed by using GraphPad Prism (version 5.00) software (GraphPad Software, San Diego, CA).

RESULTS

Neither classical nor alternative macrophage polarization is required for *Pneumocystis* clearance. To determine whether a

TABLE 1 Cellular composition of BAL fluid from transgenic mice with PcP-related IRIS[a]

Day	Strain	Mean no. of cells (10^5) $\pm$ SD					
		Total cells	Macrophages	Lymphocytes	Neutrophils	Eosinophils	DX5$^+$ cells
14	RAG2$^{-/-}$	10.9 $\pm$ 3.7	0.82 $\pm$ 0.15	1.41 $\pm$ 0.34	8.58 $\pm$ 3.73	0.16 $\pm$ 0.09	0.43 $\pm$ 0.07
	RAG2/IL-4R$\alpha^{-/-}$	4.60 $\pm$ 0.86	0.57 $\pm$ 0.19	1.47 $\pm$ 0.40	2.51 $\pm$ 0.60	0.04 $\pm$ 0.01	0.25 $\pm$ 0.07
	RAG2/IFN-γR$^{-/-}$	19.9 $\pm$ 5.76$^\#$	1.23 $\pm$ 0.24$^{*\#}$	3.52 $\pm$ 1.25	6.33 $\pm$ 1.76	7.52 $\pm$ 3.50$^{*\#}$	0.89 $\pm$ 0.31$^\#$
18	RAG2$^{-/-}$	12.7 $\pm$ 2.83	0.83 $\pm$ 0.09	3.48 $\pm$ 0.77	7.87 $\pm$ 1.59	0.19 $\pm$ 0.06	0.50 $\pm$ 0.43
	RAG2/IL-4R$\alpha^{-/-}$	9.28 $\pm$ 1.90	0.76 $\pm$ 0.15	3.61 $\pm$ 1.42	4.89 $\pm$ 1.11	0.01 $\pm$ 0.00	0.70 $\pm$ 0.35
	RAG2/IFN-γR$^{-/-}$	18.2 $\pm$ 3.11$^{*\#}$	1.23 $\pm$ 0.24$^{*\#}$	2.70 $\pm$ 1.02$^\#$	6.41 $\pm$ 1.34	6.68 $\pm$ 1.80$^{*\#}$	3.33 $\pm$ 0.51$^{*\#}$
21	RAG2$^{-/-}$	9.68 $\pm$ 1.81	2.41 $\pm$ 0.60	3.07 $\pm$ 0.59	4.00 $\pm$ 0.86	0.19 $\pm$ 0.08	1.17 $\pm$ 0.01
	RAG2/IL-4R$\alpha^{-/-}$	8.22 $\pm$ 0.71	1.34 $\pm$ 0.19	4.23 $\pm$ 0.51	2.65 $\pm$ 0.78	0.00 $\pm$ 0.00	1.30 $\pm$ 0.13
	RAG2/IFN-γR$^{-/-}$	23.6 $\pm$ 3.98$^{*\#}$	2.54 $\pm$ 0.56$^\#$	3.98 $\pm$ 0.53	11.1 $\pm$ 3.94$^{*\#}$	6.00 $\pm$ 1.92$^{*\#}$	3.53 $\pm$ 0.73$^{*\#}$
26	RAG2$^{-/-}$	10.2 $\pm$ 2.89	1.93 $\pm$ 0.41	2.89 $\pm$ 0.72	5.17 $\pm$ 2.75	0.04 $\pm$ 0.02	1.31 $\pm$ 0.43
	RAG2/IL-4R$\alpha^{-/-}$	7.03 $\pm$ 0.93	1.89 $\pm$ 0.19	2.87 $\pm$ 0.35	2.27 $\pm$ 1.18	0.00 $\pm$ 0.00	0.59 $\pm$ 0.07
	RAG2/IFN-γR$^{-/-}$	36.8 $\pm$ 12.7$^{*\#}$	3.80 $\pm$ 1.26	3.25 $\pm$ 0.66	25.4 $\pm$ 10.1$^{*\#}$	4.32 $\pm$ 1.12$^{*\#}$	5.43 $\pm$ 1.31$^{*\#}$
34	RAG2$^{-/-}$	7.80 $\pm$ 1.05	2.52 $\pm$ 0.78	1.70 $\pm$ 0.34	3.58 $\pm$ 1.38	0.00 $\pm$ 0.00	
	RAG2/IL-4R$\alpha^{-/-}$	4.88 $\pm$ 0.79	2.01 $\pm$ 0.35	1.65 $\pm$ 0.23	1.22 $\pm$ 0.70	0.00 $\pm$ 0.00	
	RAG2/IFN-γR$^{-/-}$	11.2 $\pm$ 6.70	1.15 $\pm$ 0.18*	1.12 $\pm$ 0.13	4.14 $\pm$ 2.28$^\#$	0.26 $\pm$ 0.19$^{*\#}$	

[a] Bronchoalveolar lavage fluid cells were collected from the lungs of immune-reconstituted *Pneumocystis*-infected RAG2$^{-/-}$, RAG2/IL-4R$\alpha^{-/-}$, and RAG2/IFN-γR$^{-/-}$ mice. Differential cell counts were determined by Diff-Quick staining of cytospin slides. *, $P < 0.05$ compared to RAG2$^{-/-}$ mice; $^\#$, $P < 0.05$ compared to RAG2/IL-4R$\alpha^{-/-}$ mice.

blockade of classical or alternative macrophage polarization impairs *Pneumocystis* clearance from the lungs during PcP-related IRIS, RAG2$^{-/-}$, RAG2/IFN-γR$^{-/-}$, and RAG2/IL-4R$\alpha^{-/-}$ mice were generated and infected with *Pneumocystis*. Infected mice were then immunologically reconstituted by the adoptive transfer of wild-type congenic lymphocytes to induce IRIS. This approach was used to preserve CD4$^+$ T lymphocyte function but block the cytokine-dependent polarization of alveolar macrophages. As expected, immune-reconstituted RAG2$^{-/-}$ mice cleared *Pneumocystis* infection by 4 weeks postreconstitution (Fig. 1A). Although RAG2/IFN-γR$^{-/-}$ mice had a slightly higher fungal burden at day 18 postreconstitution than did RAG2$^{-/-}$ and RAG2/IL-4R$\alpha^{-/-}$ mice, all strains cleared infection by day 34 postreconstitution without a notable difference in clearance kinetics (Fig. 1A). Measurement of anti-*Pneumocystis* serum antibodies revealed that all mice were able to produce antibodies to *Pneumocystis*. However, RAG2/IFN-γR$^{-/-}$ mice showed slightly delayed antibody production relative to RAG2$^{-/-}$ and RAG2/IL-4R$\alpha^{-/-}$ mice (Fig. 1B). The delay in antibody production by RAG2/IFN-γR$^{-/-}$ mice correlates with the higher fungal burden observed at day 18. Determination of the relative amounts of anti-*Pneumocystis* IgG1 and IgG2a isotypes in experimental IRIS mice revealed that all mouse strains were able to produce these isotypes (Fig. 1C and D). However, there appeared to be a slightly larger amount of IgG2a in the sera of immune-reconstituted RAG2/IL-4R$\alpha^{-/-}$ mice. These data demonstrate that the loss of either classical or alternative pathways of macrophage activation does not impair *Pneumocystis* clearance in a mouse model of PcP-related IRIS.

To determine whether RAG2/IFN-γR$^{-/-}$ or RAG2/IL-4R$\alpha^{-/-}$ mice displayed any overt shifts in their Th1 and Th2 responses during PcP-related IRIS, CD4$^+$ T lymphocytes from lung lavage fluid were assayed for intracellular IFN-γ and IL-4 production. There were no significant differences in the numbers of IFN-γ-producing or IL-4-producing CD4$^+$ T cells between RAG2$^{-/-}$, RAG2/IL-4R$\alpha^{-/-}$, and RAG2/IFN-γR$^{-/-}$ mice at day 14, 18, or

21 postreconstitution (Fig. 2A and B). Similar data were also found when CD4$^+$ T cells were isolated from lung homogenates. However, despite similar Th1/Th2 balances in these mice, impaired alveolar macrophage polarization was evident in the different strains. While arginase-positive macrophages were observed in RAG2$^{-/-}$ and RAG2/IFN-γR$^{-/-}$ mice, there were no identifiable arginase-positive macrophages present in RAG2/IL-4R$\alpha^{-/-}$ mice (Fig. 2C). In contrast, iNOS-positive macrophages were identified in RAG2$^{-/-}$ and RAG2/IL-4R$\alpha^{-/-}$ mice, but iNOS-positive macrophages were not detected in RAG2/IFN-γR$^{-/-}$ mice (Fig. 2D). These data demonstrate that normal CD4$^+$ T cell responses are preserved when RAG2/IFN-γR$^{-/-}$ and RAG2/IL-4R$\alpha^{-/-}$ mice are immune reconstituted with wild-type lymphocytes. However, cytokine-dependent classical and alternative macrophage polarization are blocked in RAG2/IFN-γR$^{-/-}$ and RAG2/IL-4R$\alpha^{-/-}$ mice, respectively.

Lack of IFN-γR on nonlymphocytes exacerbates PcP-related immunopathogenesis. To determine whether the blockade of either classical or alternative macrophage activation affects the development and severity of PcP-related IRIS, physiological measurements of pulmonary function were performed on immune-reconstituted RAG2$^{-/-}$, RAG2/IFN-γR$^{-/-}$, and RAG2/IL-4R$\alpha^{-/-}$ mice. Body weights and respiratory rates were monitored weekly (Fig. 3A and B). As expected, RAG2$^{-/-}$ mice developed PcP-related IRIS and lost a significant amount of body weight during the first 2 weeks postreconstitution, with a peak weight loss of ~17% at day 14. In contrast, both RAG2/IFN-γR$^{-/-}$ and RAG2/IL-4R$\alpha^{-/-}$ mice showed delayed weight loss during the first 2 weeks postreconstitution (Fig. 3A). The peak weight losses were 12% for RAG2/IFN-γR$^{-/-}$ mice and 7% for RAG2/IL-4R$\alpha^{-/-}$ mice. Mice of all three strains recovered body weight coincident with fungal clearance. While all mice displayed elevated respiratory rates following reconstitution, RAG2/IFN-γR$^{-/-}$ mice achieved significantly higher respiratory rates than those of both RAG2$^{-/-}$ and RAG2/IL-4R$\alpha^{-/-}$ mice (Fig. 3B). At day 20,

during the peak of the disease, RAG2/IFN-γR$^{-/-}$ mice exhibited an average of ~474 breaths per min. RAG2$^{-/-}$ and RAG2/IL-4Rα$^{-/-}$ mice displayed similar respiratory rates throughout disease progression and recovery (Fig. 3B). Pulmonary function measurements of dynamic lung compliance and lung resistance were performed on experimental mice at days 14, 18, 21, 26, and 34 postreconstitution. These time points were selected to represent the early, peak, and resolution phases of PcP in the IRIS model. Pulmonary function measurements are reproducible and consistent indicators of the severity of PcP. Immune-reconstituted RAG2$^{-/-}$ mice showed a typical IRIS pattern of reduced lung compliance and elevated lung resistance followed by recovery of pulmonary function as the disease resolved (Fig. 3C and D). RAG2/IL-4Rα$^{-/-}$ mice showed a very similar pattern to that of RAG2$^{-/-}$ mice, and pulmonary function measurements were not significantly different between these two groups at any time point during disease and resolution. In contrast, RAG2/IFN-γR$^{-/-}$ mice showed significantly greater IRIS-associated pulmonary function deficits than did both RAG2$^{-/-}$ and RAG2/IL-4Rα$^{-/-}$ mice. RAG2/IFN-γR$^{-/-}$ mice displayed reduced lung compliance and elevated lung resistance compared the other two strains (Fig. 3C and D), indicating that these mice suffer from exacerbated PcP-related immunopathogenesis. Importantly, despite the enhanced severity of IRIS observed in RAG2/IFN-γR$^{-/-}$ mice, they were able to recover coincident with fungal clearance.

IFN-γR signaling limits pulmonary inflammation and severity of PcP-related IRIS. Examination of hematoxylin-and-eosin-stained lung sections and enumeration of total cell numbers recovered in lavage fluid from experimental mice demonstrated that RAG2/IFN-γR$^{-/-}$ mice recruited significantly more cells to the lungs than did RAG2$^{-/-}$ and RAG2/IL-4Rα$^{-/-}$ mice at each time point following reconstitution (Table 1 and Fig. 4 and 5A). As expected, histological analyses of lung sections from immune-reconstituted RAG2$^{-/-}$ mice at day 18 postreconstitution revealed obvious cell recruitment to the alveolar spaces (Fig. 4). Examination of lung sections from RAG2/IL-4Rα$^{-/-}$ mice showed a pattern of inflammation similar to that observed in RAG2$^{-/-}$ mice. In contrast, lung sections from RAG2/IFN-γR$^{-/-}$ mice showed more intense and widespread inflammation throughout the alveoli and peribronchial regions than did those from RAG2$^{-/-}$ mice (Fig. 4). Differential staining and flow cytometry revealed that during peak disease (days 18 to 26), RAG2/IFN-γR$^{-/-}$ mice recruited more macrophages, neutrophils, eosinophils, and DX5$^+$ NK cells to the lung than did RAG2$^{-/-}$ and RAG2/IL-4Rα$^{-/-}$ mice (Table 1). RAG2$^{-/-}$ and RAG2/IL-4Rα$^{-/-}$ mice had similar numbers of macrophages, lymphocytes, and NK cells at all times. However, RAG2/IL-4Rα$^{-/-}$ mice had fewer lung eosinophils than did either RAG2$^{-/-}$ or RAG2/IFN-γR$^{-/-}$ mice (Table 1). There was no significant difference in total lavage fluid lymphocytes among the three strains. Flow cytometry assessment of T cell subsets revealed surprising results showing elevated CD4$^+$ T cell numbers but a nearly total absence of CD8$^+$ T cells in RAG2/IFN-γR$^{-/-}$ mice at all stages throughout the disease compared to RAG2$^{-/-}$ controls (Fig. 5B and C). CD8$^+$ T cells serve important suppressor and regulatory functions in the lung, and reduced CD8$^+$ T cell numbers likely contribute to exacerbated inflammation in RAG2/IFN-γR$^{-/-}$ mice. Further investigation revealed that RAG2/IFN-γR$^{-/-}$ mice were deficient in an important CD8$^+$ Foxp3$^+$ regulatory T cell subset (Fig. 5D). Thus, IFN-γR signaling
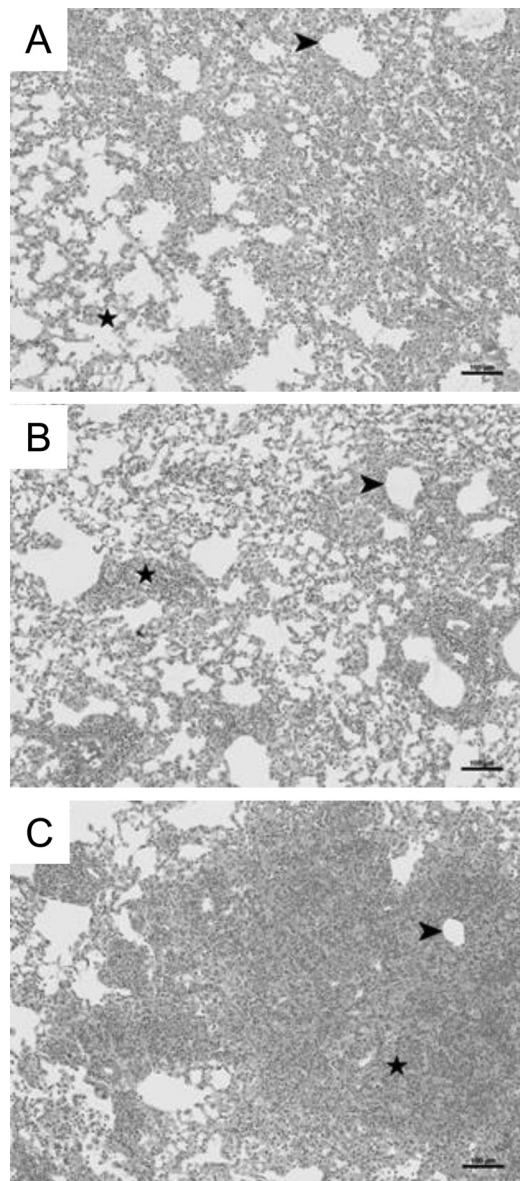

FIG 4 Loss of IFN-γR signaling is associated with increased lung inflammation. Lung sections were collected from *Pneumocystis*-infected RAG2$^{-/-}$, RAG2/IL-4Rα$^{-/-}$, and RAG2/IFN-γR$^{-/-}$ mice at day 18 post-immune reconstitution and stained with hematoxylin and eosin. Representative pictures were taken at a ×100 magnification. Arrows denote peribronchial regions, and stars denote alveolar regions.

in nonlymphocytes regulates the severity of pulmonary inflammation during PcP-related IRIS.

Dysregulated IFN-γ production in RAG2/IFN-γR$^{-/-}$ mice limits the lung CD8$^+$ T cell response during PcP. To determine whether differences in IL-4 or IFN-γ production were associated with the exacerbated IRIS observed in RAG2/IFN-γR$^{-/-}$ mice, ELISAs were performed on lung homogenate supernatants. RAG2$^{-/-}$, RAG2/IL-4Rα$^{-/-}$, and RAG2/IFN-γR$^{-/-}$ mice all had similar levels of IL-4 in the lungs during PcP-related IRIS (Fig. 6A). In contrast, we found that RAG2/IFN-γR$^{-/-}$ mice had dramatically higher lung levels of IFN-γ than did either RAG2$^{-/-}$ or RAG2/IL-4Rα$^{-/-}$ mice (Fig. 6B). To determine whether elevated
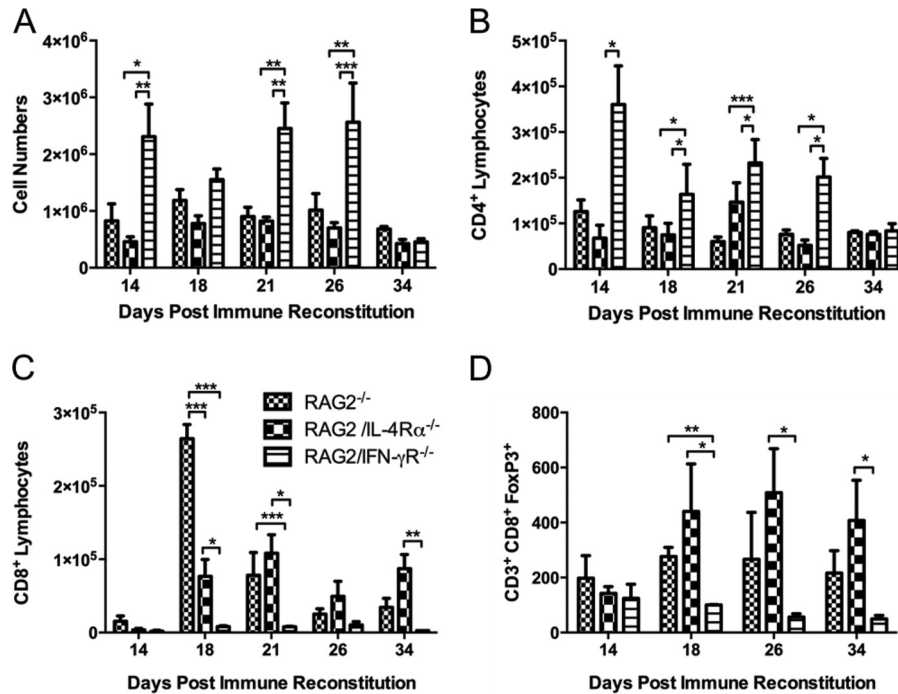
FIG 5 Loss of IFN-γR signaling is associated with increased CD4$^+$ T cell-mediated inflammation but decreased lung CD8$^+$ T cell responses. BAL fluid cells were collected from immune-reconstituted *Pneumocystis*-infected RAG2$^{-/-}$, RAG2/IL-4Rα$^{-/-}$, and RAG2/IFN-γR$^{-/-}$ mice. Total cells (A), CD4$^+$ T cells (B), CD8$^+$ T cells (C), and CD8$^+$ Foxp3$^+$ T cells (D) were enumerated by flow cytometry. Values are means ± 1 standard error ($n = 6$ to 10 per group at each time point). Data represent results from at least two independent experiments. *, $P < 0.05$; **, $P < 0.01$; ***, $P < 0.001$.

IFN-γ levels had a negative effect on the lung CD8$^+$ T cell response, *Pneumocystis*-infected RAG2/IFN-γR$^{-/-}$ mice were immune reconstituted and treated with either control antibody or anti-IFN-γ. Importantly, neutralization of IFN-γ restored the lung CD8$^+$ T cell response in RAG2/IFN-γR$^{-/-}$ mice. Anti-IFN-γ-treated mice had a >5-fold increase in the number of CD8$^+$ T cells compared to those in untreated mice (Fig. 6C). These data indicate that high levels of IFN-γ present in the lungs of RAG2/IFN-γR$^{-/-}$ mice impair the lung CD8$^+$ T cell response during PcP-related IRIS. The loss of suppressor and/or regulatory CD8$^+$ T cells may contribute to the exacerbated severity of IRIS in these mice.

DISCUSSION

A mouse model of PcP-related IRIS, in which adaptive immune function is restored following infection of immunocompromised mice, was utilized to study both fungal clearance and PcP-related immunopathogenesis. Following immune restoration in humans, symptomatic IRIS manifests as a severe inflammatory response accompanied by rapid deterioration of lung function (30). IRIS is thought to be precipitated by the recovery of CD4$^+$ T cell function, most commonly by initiating antiretroviral treatment in untreated HIV-infected patients who also have a pulmonary opportunistic infection. In the case of PcP-related IRIS, this happens as a result of recovered T cells responding to the presence of *Pneumocystis*. A recent study of a large cohort of HIV patients revealed that >10% of those who responded positively to antiretroviral treatment developed IRIS and that PcP was one of the most common IRIS-defining infections (31). Furthermore, another recent study determined that of untreated HIV patients who also had PcP

at the time of diagnosis, ~8% went on to develop IRIS (32). Clearly, the increasing frequency of PcP-related IRIS cases, combined with our inability to effectively treat severe PcP, indicates that this syndrome is a clinically significant problem.

Previous work by Wang et al. demonstrated that treatment of PcP-related IRIS with sulfasalazine (SSZ) improved lung physiology, reduced lung inflammation, accelerated fungal clearance, and enhanced the resolution of IRIS. Importantly, the beneficial effects of SSZ on inflammation and fungal clearance were associated with its ability to promote an alternatively activated alveolar macrophage phenotype (18). The protective role of Th2 responses and alternatively activated macrophages against *Pneumocystis* infection has also been demonstrated in previous studies (22, 33). While these data suggest that alternatively activated M2a macrophages possess anti-*Pneumocystis* effector function, the requirement for either classical or alternatively activated macrophages for the clearance of *Pneumocystis* during IRIS has not been determined. In order to investigate the function of specific macrophage subsets in contributing to host defense and/or immunopathogenesis during PcP, we generated RAG-deficient mice with distinct restrictions in polarizing either M1 (RAG2/IFN-γR$^{-/-}$) or M2 (RAG2/IL-4Rα$^{-/-}$) macrophages. Using these mice, we were able to model IRIS in mice that possess wild-type lymphocytes but have macrophages which are unable to respond to polarizing Th effector cytokines. Importantly, our data showed that during PcP-related IRIS, all strains of mice were able to clear *Pneumocystis* effectively regardless of their ability to polarize macrophages to an M1 or M2 phenotype. Immune-reconstituted RAG2/IL-4Rα$^{-/-}$ mice exhibited similar rates of *Pneumocystis* clearance despite lacking arginase-positive M2 macrophages. RAG2/IFN-γR$^{-/-}$
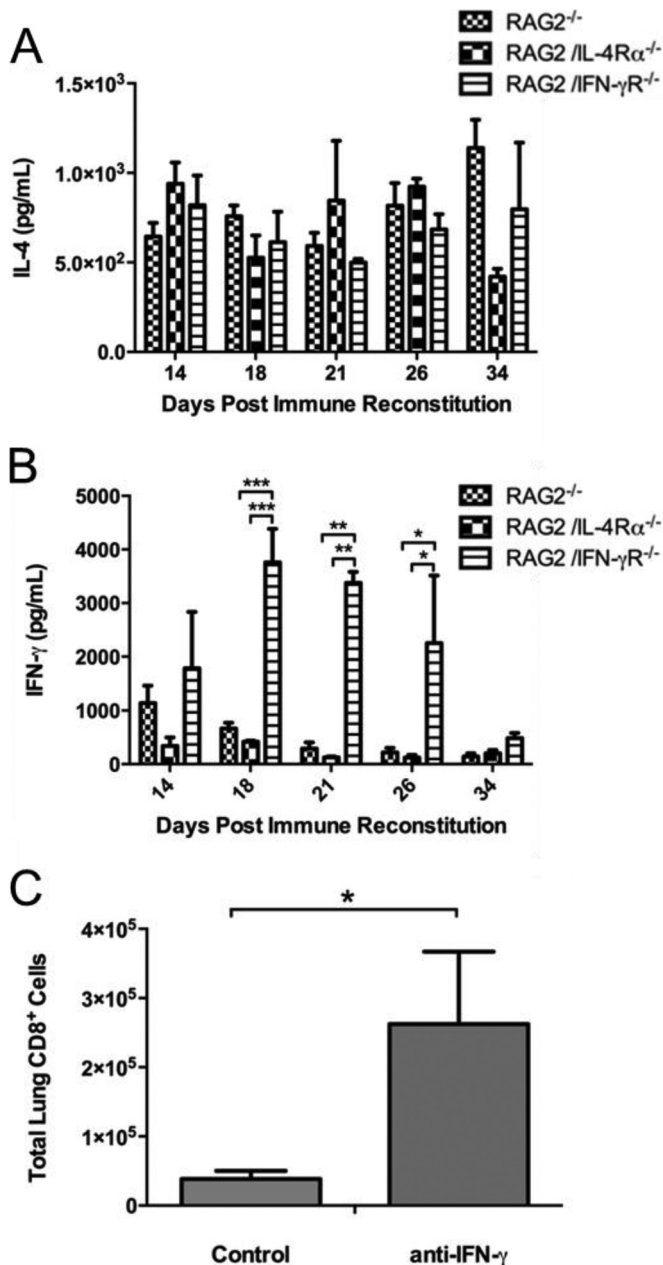
FIG 6 Excessive IFN-γ production impairs the CD8⁺ T cell response during
PcP-related IRIS. (A and B) IL-4 (A) and IFN-γ (B) levels in the lung homog-
enates from immune-reconstituted *Pneumocystis*-infected RAG2$^{-/-}$, RAG2/
IL-4Rα$^{-/-}$, and RAG2/IFN-γR$^{-/-}$ mice were measured (n = 6 to 10 per
group at each time point). (C) In a separate experiment, *Pneumocystis*-infected
RAG2/IFN-γR$^{-/-}$ mice were immune reconstituted and treated with either
anti-IFN-γ or control rat IgG beginning at day 3 postreconstitution. At day 18
postreconstitution, the mice were sacrificed, and lung CD8⁺ T cell numbers
were determined by flow cytometry. Values are means ± 1 standard error (n =
4 to 5 per group at each time point). *, $P < 0.05$; **, $P < 0.01$; ***, $P < 0.001$.

mice lacked iNOS-positive M1 macrophages but also cleared
Pneumocystis similarly to reconstituted RAG2 mice (Fig. 1 and 2).
These data provide direct evidence that neither M1 nor M2 mac-
rophages are required for *Pneumocystis* clearance during IRIS. It is
possible that the presence of either M1 or M2 macrophages is
sufficient to clear *Pneumocystis* from the lung and that a loss of one

subset is compensated for by the presence of the other. Alterna-
tively, it is possible that CD4⁺ T cell-dependent activation of mac-
rophages during the immune response to *Pneumocystis* proceeds
via a mechanism that is independent of classical or alternative
activation. For example, antibody- or complement-mediated op-
sonization of *Pneumocystis* could represent a key mechanism by
which CD4⁺ T cells promote macrophage phagocytosis of *Pneu-
mocystis*. It is noteworthy that all three strains of mice were able to
produce anti-*Pneumocystis* antibodies during IRIS (Fig. 1). There
is also the possibility that there are other mechanisms of CD4-
dependent macrophage polarization that do not require signaling
through IFN-γR or IL-4Rα.

Although CD4⁺ T cells are required for host defense against
Pneumocystis, they also contribute to lung injury and immuno-
pathogenesis during PcP (23). The severity of lung damage sus-
tained during PcP-related IRIS is directly related to the host's
CD4⁺ T cell-mediated immune response, and IFN-γ is thought to
be one of the cytokines that drive IRIS. Thus, we hypothesized that
a loss of IFN-γR signaling in macrophages would dampen PcP-
related immunopathogenesis. Initially, our noninvasive measure-
ments of weight loss supported this hypothesis by showing that
immune-reconstituted RAG2/IFN-γR$^{-/-}$ mice lost less weight
than did RAG2$^{-/-}$ mice. However, this was contradicted by data
showing that immune-reconstituted RAG2/IFN-γR$^{-/-}$ mice
displayed exacerbated PcP-related lung injury and respiratory im-
pairment (Fig. 3 to 5). Both the intensity of pulmonary inflamma-
tion and the pulmonary function deficits associated with PcP-
associated IRIS were dramatically amplified in RAG2/IFN-γR$^{-/-}$
mice compared to RAG2$^{-/-}$ mice. The specific reason why RAG2/
IFN-γR$^{-/-}$ mice displayed less weight loss but exacerbated IRIS
relative to RAG2$^{-/-}$ mice is unclear. However, we speculate that
the loss of the IFN-γ receptor attenuated IRIS-related systemic
inflammation but caused enhanced inflammation in the local lung
environment. These findings highlight the complexity of IRIS and
suggest that systemic and local responses are differentially regu-
lated during the progression of this disease.

Despite the general enhancement of inflammatory cell recruit-
ment to the lungs of RAG2/IFN-γR$^{-/-}$ mice, these mice showed a
severe defect in the lung CD8⁺ T cell response (Fig. 5). Data from
previous reports by Swain et al. and Bhagwat et al. are consistent
with our observation of exacerbated CD4⁺ T cell-mediated IRIS
when CD8⁺ T cells are absent during recovery of host immune
function (16, 27). Although CD8⁺ T cells have long been regarded
as cytotoxic cells, the CD8⁺ T cells recruited to the lung during
IRIS appear to play a more regulatory role by limiting the CD4⁺ T
cell response to *Pneumocystis* infection (34, 35). Similarly, the im-
mune-regulatory role of CD8⁺ T cells has also been observed for
allergic asthma, where the depletion of CD8⁺ T cells amplified the
inflammatory response and promoted eosinophil accumulation
in the airways (36, 37). The absence of CD8⁺ T cells in the lungs of
RAG2/IFN-γR$^{-/-}$ mice in our study also reflects a reduction in
the frequency of Foxp3⁺ CD8⁺ T regulatory cells in these mice
(Fig. 5). Similar functional properties have been found for CD8⁺
and CD4⁺ T regulatory cells (38, 39), which include limiting an
ongoing immune response (40, 41). Thus, our findings suggest
that IFN-γR signaling regulates the intensity of the CD4 response
during PcP-related IRIS by promoting the recruitment of CD8⁺
regulatory or suppressor cells. It should be noted that despite the
increased severity of PcP-related IRIS in immune-reconstituted
RAG2/IFN-γR$^{-/-}$ mice, these mice were able to fully resolve their

pulmonary inflammation even in the absence of CD8$^+$ T suppressor or regulatory cells in the lung. It is likely that resolution in these mice resulted from a combination of fungal clearance, which removes the *Pneumocystis* antigen that drives the inflammatory response, and the function of CD4$^+$ T regulatory cells. In this model of PcP-related IRIS, CD8$^+$ T cells appear to control the intensity but not necessarily the duration of the CD4$^+$ T cell-mediated pulmonary immune response.

RAG2/IFN-γR$^{-/-}$ mice displayed exacerbated PcP-related IRIS, which was associated with impaired lung CD8$^+$ T cell responses and significantly elevated levels of IFN-γ in the lungs compared to those in RAG2$^{-/-}$ and RAG2/IL-4Rα$^{-/-}$ mice (Fig. 6). In order to explore the mechanism by which the loss of IFN-γR signaling in nonlymphocytes causes impaired lung CD8$^+$ T cell responses during PcP-related IRIS, *Pneumocystis*-infected RAG2/IFN-γR$^{-/-}$ mice were immune reconstituted and treated with either control antibody or anti-IFN-γ antibody. Neutralization of IFN-γ restored lung CD8$^+$ T cell responses in RAG2/IFN-γR$^{-/-}$ mice, indicating that excessive IFN-γ production negatively regulates the CD8$^+$ T cell response during PcP-related IRIS. We speculate that the source of excessive IFN-γ is likely NK cells, which are capable of producing large amounts of IFN-γ and also express IFN-γR. Importantly, we found that RAG2/IFN-γR$^{-/-}$ mice showed dramatic increases in the numbers of NK cells in the lungs during PcP-related IRIS (Table 1). Thus, we suspect that the loss of IFN-γR on NK cells in RAG2/IFN-γR$^{-/-}$ mice disrupts a negative-feedback mechanism, resulting in elevated numbers of IFN-γ-producing NK cells in the lung. Furthermore, as shown in Fig. 6, elevated levels of IFN-γ suppress the lung CD8$^+$ T cell response during PcP-related IRIS. While these findings help to explain the mechanisms of impaired CD8$^+$ T cell responses in RAG2/IFN-γR$^{-/-}$ mice, they clearly raise more questions regarding how IFN-γ, NK cells, and CD8$^+$ T cells interact during PcP-related IRIS.

In summary, while prior work suggests that an enhancement of M2 polarization accelerates *Pneumocystis* clearance and promotes disease resolution (18, 22), our present findings demonstrate that restricting the ability of macrophages to polarize to either an M1 or M2 phenotype does not affect the ability of mice to clear *Pneumocystis* infection. Instead, the loss of IFN-γR signaling exacerbates *Pneumocystis* immunopathogenesis, which is likely related to the impaired recruitment of CD8$^+$ T cell suppressor cells to the lung.

ACKNOWLEDGMENTS

REFERENCES

1. **Vargas SL, Hughes WT, Santolaya ME, Ulloa AV, Ponce CA, Cabrera CE, Cumsille F, Gigliotti F.** 2001. Search for primary infection by *Pneumocystis carinii* in a cohort of normal, healthy infants. Clin Infect Dis **32**:855–861. http://dx.doi.org/10.1086/319340.

2. **Beck JM, Warnock ML, Curtis JL, Sniezek MJ, Arraj-Peffer SM, Kaltreider HB, Shellito JE.** 1991. Inflammatory responses to *Pneumocystis carinii* in mice selectively depleted of helper T lymphocytes. Am J Respir Cell Mol Biol **5**:186–197. http://dx.doi.org/10.1165/ajrcmb/5.2.186.

3. **Radhi S, Alexander T, Ukwu M, Saleh S, Morris A.** 2008. Outcome of HIV-associated *Pneumocystis* pneumonia in hospitalized patients from 2000 through 2003. BMC Infect Dis **8**:118. http://dx.doi.org/10.1186/1471-2334-8-118.

4. **Kaur N, Mahl TC.** 2007. *Pneumocystis jiroveci* (*carinii*) pneumonia after infliximab therapy: a review of 84 cases. Dig Dis Sci **52**:1481–1484. http://dx.doi.org/10.1007/s10620-006-9250-x.

5. **Hardak E, Oren I, Dann EJ, Yigla M, Faibish T, Rowe JM, Avivi I.** 2012. The increased risk for *Pneumocystis* pneumonia in patients receiving rituximab-CHOP-14 can be prevented by the administration of trimethoprim/sulfamethoxazole: a single-center experience. Acta Haematol **127**:110–114. http://dx.doi.org/10.1159/000334113.

6. **Sivam S, Sciurba FC, Lucht LA, Zhang Y, Duncan SR, Norris KA, Morris A.** 2011. Distribution of *Pneumocystis jirovecii* in lungs from colonized COPD patients. Diagn Microbiol Infect Dis **71**:24–28. http://dx.doi.org/10.1016/j.diagmicrobio.2011.05.008.

7. **Mason GR, Hashimoto CH, Dickman PS, Foutty LF, Cobb CJ.** 1989. Prognostic implications of bronchoalveolar lavage neutrophilia in patients with *Pneumocystis carinii* pneumonia and AIDS. Am Rev Respir Dis **139**:1336–1342. http://dx.doi.org/10.1164/ajrccm/139.6.1336.

8. **Benfield TL, Van Steenwijk R, Nielsen TL, Dichter JR, Lipschik GY, Jensen BN, Junge J, Shelhamer JH, Lundgren JD.** 1995. Interleukin-8 and eicosanoid production in the lung during moderate to severe *Pneumocystis carinii* pneumonia in AIDS: a role of interleukin-8 in the pathogenesis of P. carinii pneumonia. Respir Med **89**:285–290. http://dx.doi.org/10.1016/0954-6111(95)90089-6.

9. **Jensen BN, Lisse IM, Gerstoft J, Borgeskov S, Skinhoj P.** 1991. Cellular profiles in bronchoalveolar lavage fluid of HIV-infected patients with pulmonary symptoms: relation to diagnosis and prognosis. AIDS **5**:527–533. http://dx.doi.org/10.1097/00002030-199105000-00008.

10. **Limper AH, Offord KP, Smith TF, Martin WJ, II.** 1989. *Pneumocystis carinii* pneumonia. Differences in lung parasite number and inflammation in patients with and without AIDS. Am Rev Respir Dis **140**:1204–1209.

11. **Bonham S, Meya DB, Bohjanen PR, Boulware DR.** 2008. Biomarkers of HIV immune reconstitution inflammatory syndrome. Biomark Med **2**:349–361. http://dx.doi.org/10.2217/17520363.2.4.349.

12. **Barry SM, Lipman MC, Deery AR, Johnson MA, Janossy G.** 2002. Immune reconstitution pneumonitis following *Pneumocystis carinii* pneumonia in HIV-infected subjects. HIV Med **3**:207–211. http://dx.doi.org/10.1046/j.1468-1293.2002.00115.x.

13. **Masur H, Ognibene FP, Yarchoan R, Shelhamer JH, Baird BF, Travis W, Suffredini AF, Deyton L, Kovacs JA, Falloon J, Davey R, Polis M, Metcalf J, Baseler M, Wesley R, Gill VJ, Fauci AS, Lane HC.** 1989. CD4 counts as predictors of opportunistic pneumonias in human immunodeficiency virus (HIV) infection. Ann Intern Med **111**:223–231. http://dx.doi.org/10.7326/0003-4819-111-3-223.

14. **Roths JB, Sidman CL.** 1992. Both immunity and hyperresponsiveness to *Pneumocystis carinii* result from transfer of CD4$^+$ but not CD8$^+$ T cells into severe combined immunodeficiency mice. J Clin Invest **90**:673–678. http://dx.doi.org/10.1172/JCI115910.

15. **Shellito JE, Tate C, Ruan S, Kolls J.** 2000. Murine CD4$^+$ T lymphocyte subsets and host defense against *Pneumocystis carinii*. J Infect Dis **181**:2011–2017. http://dx.doi.org/10.1086/315487.

16. **Swain SD, Meissner NN, Harmsen AG.** 2006. CD8 T cells modulate CD4 T-cell and eosinophil-mediated pulmonary pathology in *Pneumocystis* pneumonia in B-cell-deficient mice. Am J Pathol **168**:466–475. http://dx.doi.org/10.2353/ajpath.2006.050724.

17. **Mantovani A, Sica A, Sozzani S, Allavena P, Vecchi A, Locati M.** 2004. The chemokine system in diverse forms of macrophage activation and polarization. Trends Immunol **25**:677–686. http://dx.doi.org/10.1016/j.it.2004.09.015.

18. **Wang J, Gigliotti F, Bhagwat SP, George TC, Wright TW.** 2010. Immune modulation with sulfasalazine attenuates immunopathogenesis but enhances macrophage-mediated fungal clearance during *Pneumocystis* pneumonia. PLoS Pathog **6**:e1001058. http://dx.doi.org/10.1371/journal.ppat.1001058.

19. **Keegan AD, Johnston JA, Tortolani PJ, McReynolds LJ, Kinzer C, O'Shea JJ, Paul WE.** 1995. Similarities and differences in signal transduction by interleukin 4 and interleukin 13: analysis of Janus kinase activation. Proc Natl Acad Sci U S A **92**:7681–7685. http://dx.doi.org/10.1073/pnas.92.17.7681.

20. **Paliard X, de Waal Malefijt R, Yssel H, Blanchard D, Chretien I, Abrams J, de Vries J, Spits H.** 1988. Simultaneous production of IL-2, IL-4, and IFN-gamma by activated human CD4$^+$ and CD8$^+$ T cell clones. J Immunol **141**:849–855.

21. **Stein M, Keshav S, Harris N, Gordon S.** 1992. Interleukin 4 potently

enhances murine macrophage mannose receptor activity: a marker of alternative immunologic macrophage activation. J Exp Med **176:**287–292. http://dx.doi.org/10.1084/jem.176.1.287.

22. **Nelson MP, Christmann BS, Werner JL, Metz AE, Trevor JL, Lowell CA, Steele C.** 2011. IL-33 and M2a alveolar macrophages promote lung defense against the atypical fungal pathogen *Pneumocystis murina*. J Immunol **186:**2372–2381. http://dx.doi.org/10.4049/jimmunol.1002558.

23. **Wright TW, Gigliotti F, Finkelstein JN, McBride JT, An CL, Harmsen AG.** 1999. Immune-mediated inflammation directly impairs pulmonary function, contributing to the pathogenesis of *Pneumocystis carinii* pneumonia. J Clin Invest **104:**1307–1317. http://dx.doi.org/10.1172/JCI6688.

24. **Shinkai Y, Rathbun G, Lam KP, Oltz EM, Stewart V, Mendelsohn M, Charron J, Datta M, Young F, Stall AM, Alt FW.** 1992. RAG-2-deficient mice lack mature lymphocytes owing to inability to initiate V(D)J rearrangement. Cell **68:**855–867. http://dx.doi.org/10.1016/0092-8674(92)90029-C.

25. **Wang J, Gigliotti F, Maggirwar S, Johnston C, Finkelstein JN, Wright TW.** 2005. *Pneumocystis carinii* activates the NF-kappaB signaling pathway in alveolar epithelial cells. Infect Immun **73:**2766–2777. http://dx.doi.org/10.1128/IAI.73.5.2766-2777.2005.

26. **Kelly-Welch AE, Melo ME, Smith E, Ford AQ, Haudenschild C, Noben-Trauth N, Keegan AD.** 2004. Complex role of the IL-4 receptor alpha in a murine model of airway inflammation: expression of the IL-4 receptor alpha on nonlymphoid cells of bone marrow origin contributes to severity of inflammation. J Immunol **172:**4545–4555. http://dx.doi.org/10.4049/jimmunol.172.7.4545.

27. **Bhagwat SP, Gigliotti F, Xu H, Wright TW.** 2006. Contribution of T cell subsets to the pathophysiology of *Pneumocystis*-related immunorestitution disease. Am J Physiol Lung Cell Mol Physiol **291:**L1256–L1266. http://dx.doi.org/10.1152/ajplung.00079.2006.

28. **An CL, Gigliotti F, Harmsen AG.** 2003. Exposure of immunocompetent adult mice to *Pneumocystis carinii* f. sp. *muris* by cohousing: growth of *P. carinii* f. sp. *muris* and host immune response. Infect Immun **71:**2065–2070.

29. **Chen W, Havell E, Gigliotti F, Harmsen AG.** 1993. Interleukin-6 production in a murine model of *Pneumocystis carinii* pneumonia: relation to resistance and inflammatory response. Infect Immun **61:**97–102.

30. **Cheng VC, Hung IF, Wu AK, Tang BS, Chu CM, Yuen KY.** 2004. Lymphocyte surge as a marker for immunorestitution disease due to *Pneumocystis jiroveci* pneumonia in HIV-negative immunosuppressed hosts. Eur J Clin Microbiol Infect Dis **23:**512–514. http://dx.doi.org/10.1007/s10096-004-1140-6.

31. **Novak RM, Richardson JT, Buchacz K, Chmiel JS, Durham MD, Palella FJ, Wendrow A, Wood K, Young B, Brooks JT.** 2012. Immune reconstitution inflammatory syndrome: incidence and implications for mortality. AIDS **26:**721–730. http://dx.doi.org/10.1097/QAD.0b013e3283511e91.

32. **Grant PM, Komarow L, Andersen J, Sereti I, Pahwa S, Lederman MM, Eron J, Sanne I, Powderly W, Hogg E, Suckow C, Zolopa A.** 2010. Risk factor analyses for immune reconstitution inflammatory syndrome in a randomized study of early vs. deferred ART during an opportunistic infection. PLoS One **5:**e11416. http://dx.doi.org/10.1371/journal.pone.0011416.

33. **Myers RC, Dunaway CW, Nelson MP, Trevor JL, Morris A, Steele C.** 2013. STAT4-dependent and -independent Th2 responses correlate with protective immunity against lung infection with *Pneumocystis murina*. J Immunol **190:**6287–6294. http://dx.doi.org/10.4049/jimmunol.1300431.

34. **Jones HP, Tabor L, Sun X, Woolard MD, Simecka JW.** 2002. Depletion of CD8+ T cells exacerbates CD4+ Th cell-associated inflammatory lesions during murine mycoplasma respiratory disease. J Immunol **168:**3493–3501. http://dx.doi.org/10.4049/jimmunol.168.7.3493.

35. **Kemeny DM, Noble A, Holmes BJ, Diaz-Sanchez D.** 1994. Immune regulation: a new role for the CD8+ T cell. Immunol Today **15:**107–110. http://dx.doi.org/10.1016/0167-5699(94)90152-X.

36. **Allakhverdi Z, Lamkhioued B, Olivenstein R, Hamid Q, Renzi PM.** 2000. CD8 depletion-induced late airway response is characterized by eosinophilia, increased eotaxin, and decreased IFN-gamma expression in rats. Am J Respir Crit Care Med **162:**1123–1131. http://dx.doi.org/10.1164/ajrccm.162.3.9910001.

37. **Laberge S, Wu L, Olivenstein R, Xu LJ, Renzi PM, Martin JG.** 1996. Depletion of CD8+ T cells enhances pulmonary inflammation but not airway responsiveness after antigen challenge in rats. J Allergy Clin Immunol **98:**617–627. http://dx.doi.org/10.1016/S0091-6749(96)70096-9.

38. **Cosmi L, Liotta F, Lazzeri E, Francalanci M, Angeli R, Mazzinghi B, Santarlasci V, Manetti R, Vanini V, Romagnani P, Maggi E, Romagnani S, Annunziato F.** 2003. Human CD8+CD25+ thymocytes share phenotypic and functional features with CD4+CD25+ regulatory thymocytes. Blood **102:**4107–4114. http://dx.doi.org/10.1182/blood-2003-04-1320.

39. **Kim HJ, Verbinnen B, Tang X, Lu L, Cantor H.** 2010. Inhibition of follicular T-helper cells by CD8(+) regulatory T cells is essential for self tolerance. Nature **467:**328–332. http://dx.doi.org/10.1038/nature09370.

40. **Joosten SA, Ottenhoff TH.** 2008. Human CD4 and CD8 regulatory T cells in infectious diseases and vaccination. Hum Immunol **69:**760–770. http://dx.doi.org/10.1016/j.humimm.2008.07.017.

41. **Aandahl EM, Torgersen KM, Tasken K.** 2008. CD8+ regulatory T cells—a distinct T-cell lineage or a transient T-cell phenotype? Hum Immunol **69:**696–699. http://dx.doi.org/10.1016/j.humimm.2008.08.291.